Arab J Sci Eng (2015) 40:2701–2709
DOI 10.1007/s13369-015-1747-1

RESEARCH ARTICLE - MECHANICAL ENGINEERING

Microstructure and Mechanical Properties of ZTA Ceramic-Lined Composite Pipe Prepared by Centrifugal-SHS

J. An[1] · J. Zhao[1] · Z. G. Su[2] · Z. Wen[1] · D. S. Xu[1]

Received: 4 January 2015 / Accepted: 7 June 2015 / Published online: 24 June 2015

Abstract A type of zirconia-toughened alumina (ZTA) ceramic-lined composite steel pipe was fabricated by using self-propagation high-temperature synthesis and centrifugal casting technique. The microstructure and phase constituents of ZTA ceramic layer were analyzed by means of optical microscope, scanning electron microscope and X-ray diffractometer (XRD). The fracture toughness of ceramic layers and mechanical shock of Al_2O_3 and ZTA ceramic-lined composite pipes were measured using Vickers indentation microfracture method and the repetitive impacting method. The results show that the phase constituents of ZTA ceramic layer were Al_2O_3, $FeAl_2O_4$ and t-ZrO_2 phases, and no m-ZrO_2 phase was detected by XRD. Addition of ZrO_2 reduced the width of Al_2O_3 dendrites and led to formation of a microstructure with fine ZrO_2 particles distributed at boundaries of Al_2O_3 dendrites. The fracture toughness was increased from 0.56 MPa $m^{1/2}$ of Al_2O_3 ceramic layer to 5.74 MPa $m^{1/2}$ of ZTA ceramic layer. The mechanical shock resistance at the center of the ceramic-lined composite pipe was increased from twice to 19 times after addition of ZrO_2 into the Al_2O_3 matrix.

Keywords SHS · Ceramic lining · Microstructure · Fracture toughness

✉ D. S. Xu
xudeshengjlu2000@163.com

[1] Key Laboratory of Automobile Materials, Ministry of Education, Department of Materials, Science and Engineering, Jilin University, Changchun 130025, China

[2] State Key Laboratory of New Ceramics and Fine Processing, School of Materials Science and Engineering, Tsinghua University, Beijing 100084, China

1 Introduction

Self-propagation high-temperature synthesis (SHS) is a new technique for material synthesis. It has so many attractive advantages such as low energy consumption, short reaction time, high production quantity and light environmental pollution [1–4]. One of the most important applications of SHS is to produce ceramic-lined composite steel pipes by combining with centrifugal casting technique (C–T). Odawara et al. [5] successfully developed 5.5-m-long ceramic-lined composite steel pipe, which consisted of the innermost ceramic layer of Al_2O_3, Fe-rich layer and the outer steel substrate pipe. The Fe-rich layer and Al_2O_3 ceramic layer were reported to be mechanically interlocked by a mosaic structure [6]. The ceramic-lined composite steel pipes produced by SHS CT method have been extensively used in many military and industrial applications such as gun barrel, transportation of coal cinder, mineral powder, limestone flour and oil-water mixture [7–9], because the thick coated ceramic layers on the inner surfaces of pipes enable them to apply in severe conditions where high resistance to abrasion, corrosion, erosion and heat is required. However, the instinct brittleness of the ceramic layer poses a series of problems which make the ceramic-lined composite steel pipes (CLCPs) to be treated unlike the commonly used steel pipes, because much carefulness must be taken to avoid the cracks or fragmentation of the ceramic layer in processes of machining screw thread at ends of pipes, transportation and installation. Therefore, improvement of toughness and mechanical shock resistance of the ceramic layer is a key to further application of the CLCPs.

It is well known that the toughness of alumina (Al_2O_3) ceramics can be considerably increased by the incorporation of fine zirconia (ZrO_2) particles [10–12]. The toughening

mechanisms associated with zirconia toughening alumina are mainly based on the stress-induced tetragonal → monoclinic martensite transformation and microcracks. In these toughening mechanisms, the main toughening origin is to maintain as much as possible amount of tetragonal zirconia phase particles dispersed in alumina matrix. However, the volume ratio of tetragonal phase to monoclinic phase is usually not very high in ZTA ceramics produced using conventional sintering route due to the high transformation temperature of tetragonal → monoclinic martensite around 1000 °C. Several sol-gel processes have been used to prepare ZrO_2 powder which retains a substantial amount of tetragonal zirconia even after annealing at 1000 °C. Kaya and Butler [13] produced a high-strength (1270 MPa) and tough (>9 MPa $m^{1/2}$) zirconia-toughened alumina ceramics from sol-derived pastes comprising a mixture of boehmite (γ-AlOOH) and nano-size zirconia powders using extrusion. Rao et al. [14] produced the metastable t-ZrO_2 in Al_2O_3-15 wt% ZrO_2 powder calcined at 600 °C and obtained high fracture toughness of 8.5 MPa $m^{1/2}$ after sintering at 1475 °C.

By comparison, toughening alumina with various partially stabilized zirconias (PSZ) is an easy and practical method. The toughening of alumina by dispersing zirconia particles was first encountered by the development of the PSZ [15], which enables an amount of zirconia particles to remain in the state of tetragonal phase in alumina matrix. Since then, there has been extensive research into both the fabrication and the mechanical property–microstructure relationship of alumina with dispersed PSZ. Becher [16] fabricated alumina containing Y_2O_3 partially stabilized zirconia by conventional sintering, which had fracture toughness as high as 10 $MPa^{1/2}$.

During the centrifugal-SHS preparation of the CLCP, the ceramic layer and Fe-rich layer solidify at different temperatures, a large difference in coefficient of thermal expansion between the two layers arouses a unique residual thermal stress distribution, the steel substrate pipe is subjected to residual tensile stress, while the ceramic layer and Fe-rich layer suffer from residual compressive stress. The compressive stress is reported to be beneficial for zirconia to be retained in metastable tetragonal form [17]. Therefore, it is expected that a high toughness of ceramic layer may be obtained in CLCP produced by SHS CT method. Moreover, only little work has been made on investigation of microstructure and properties of centrifugal-SHS composite pipe by addition of zirconia in the alumina ceramic layer.

In this paper, we report the use of 3 mol% Y_2O_3-doped ZrO_2 powders to prepare a type of ZTA CLCP by centrifugal-SHS process, which has high fracture toughness and mechanical shock resistance. The microstructure and properties of the ZTA CLCP are investigated.

2 Experimental Methods

2.1 Preparation of CLCPs with Centrifugal Casting Technique

A J55 steel oil pipe with 73.02 mm diameter and 5.51 mm wall thickness was cut into pieces of 400 mm length for usage of centrifugal-SHS process. The chemical composition of J55 steel is listed in Table 1. Two kinds of thermit powder mixtures were prepared by blending Al and F_2O_3 powders for Al_2O_3 CLCP and Al, F_2O_3 and 3 mol% Y_2O_3-doped ZrO_2 powders for ZTA CLCP. ZrO_2 powders doped by 3 mol% Y_2O_3 were prepared by a titration reaction process. They were provided by Yixin 3-Science Ultra-fine Powder Co., Ltd., China. The addition amount of ZrO_2 was 6 wt% of Al + F_2O_3 powders. The chemical mole ratio of the Al and F_2O_3 powders conformed to the following chemical reaction:

$$F_2O_3 + 2Al = Al_2O_3 + 2Fe + 836\ \text{kJ/mol} \quad (1)$$

The J55 steel pipe was loaded with the thermit mixture and placed horizontally on the SHS-centrifugal apparatus. Figure 1 is the photograph of SHS-centrifugal apparatus used in the present study. When the required rotational velocity of the centrifuge machine is reached, the thermit mixture was ignited by a tungsten filament. The reaction as described in Eq. (1) emitted an enormous amount of heat, and the temperature of the system immediately increased to about 2500 K.

Table 1 Chemical composition of J55 steel oil pipe

Element	C	Si	Mn	P	S	Al	V
wt%	0.370	0.240	1.290	0.013	0.006	0.040	0.015

Fig. 1 Photograph of SHS-centrifugal apparatus used in the present study

The SHS reaction took a very short period less than a second accompanied by a roar of the reaction. Upon the completion of the reaction, the surface color of CLCP changed from the bright yellow into the dark red as time went on; meanwhile, the centrifuge apparatus continued to run for 10 more minutes until the CLCP cooled down.

2.2 Microstructures of Ceramic-Lined Composite Steel Pipes

The phase constituents of Al_2O_3 and ZTA ceramic layers were analyzed by XRD. The amount of ZrO_2 monoclinic phase (X_m) is determined using the following relation [18]:

$$X_m = \frac{I(111)_m + I(11\bar{1})_m}{I(111)_m + I(11\bar{1})_m + I(111)_t} \tag{2}$$

where m refers to the intensity of ZrO_2 monoclinic phase peaks and t refers to ZrO_2 tetragonal phase peaks.

The microstructures of Al_2O_3 and ZTA ceramic layers were observed under a LEXT-OLS3000 confocal scanning laser microscope.

2.3 Properties of Ceramic-Lined Composite Steel Pipes

The Vickers hardness of ceramic layers was determined using a load of 500 g for a dwell period of 15 s. The crushing strength of Al_2O_3 and ZTA CLCPs was measured using MTS810 material test system. In the crushing test, a piece of pipe of 50 mm length was compressed in the radial direction as shown in Fig. 2. The crushing strength was calculated according to Odawara's formula [19]

$$\sigma_F = \frac{F}{Lt} \times \frac{1}{\pi(1+k)} \times \left\{1 + \frac{1}{k}\left(\frac{t}{D+t}\right)\right\} \tag{3}$$

where L, t and D are the length, thickness and average diameter of the test pipe, respectively, F is the turning point load deviated from straight line at the compress load—displacement curve, and k is a cross section factor.

$$k = 1 + \frac{D}{2t} \times \ln\left[\frac{D+t}{D-t}\right] \tag{4}$$

The fracture toughness of ceramic layer K_{IC} was obtained through Vickers indentation microfracture method, which correlates K_{IC} with the length of cracks emanating from the Vickers indentation corners. The Vickers indentation was obtained using a load of 10 kg for a dwell period of 15 s. The fracture toughness can be calculated using the following equations [20]:

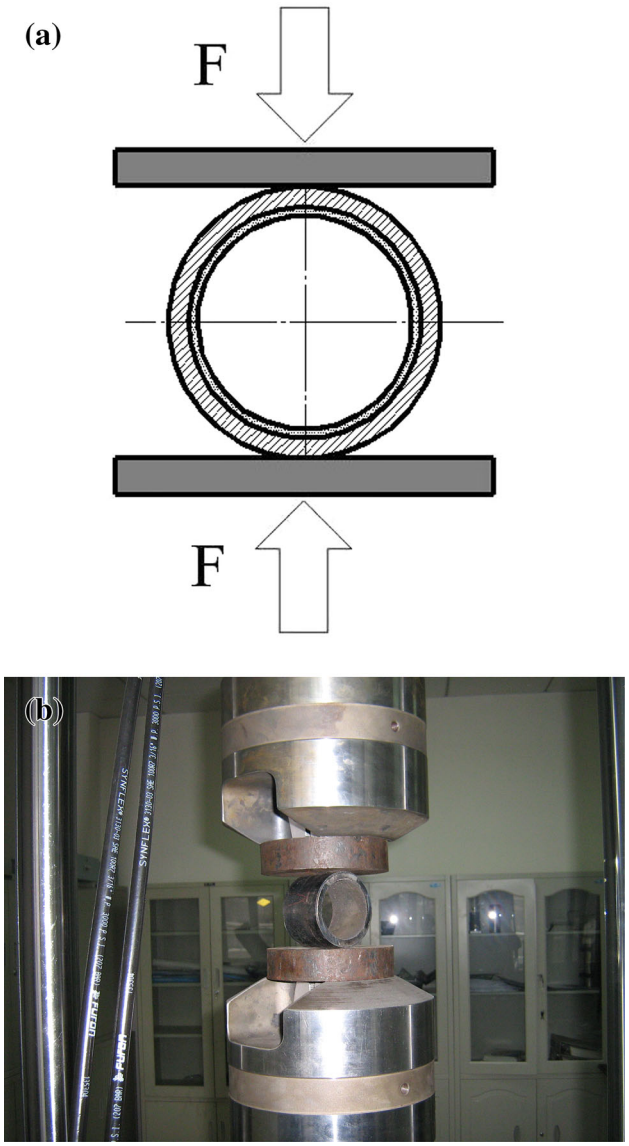

Fig. 2 Schematic diagram (**a**) and photograph (**b**) of the compression test

$$\left(\frac{3K_{IC}}{Ha^{1/2}}\right)\left(\frac{H}{3E}\right)^{2/5} = 0.035\left(\frac{l}{a}\right)^{-1/2} \quad \left(0.25 \le \frac{l}{a} \le 2.5\right) \tag{5}$$

$$\left(\frac{3K_{IC}}{Ha^{1/2}}\right)\left(\frac{H}{3E}\right)^{2/5} = 0.129\left(\frac{l}{a}\right)^{-3/2} \quad \left(\frac{l}{a} \ge 2.5\right) \tag{6}$$

where E and H are, respectively, the Young's modulus and Vickers hardness values, a is the half-diagonal of the Vickers indent, c is the radius of surface crack, and l is the length of a crack.

The mechanical shock was measured using the repetitive impacting method. The mechanical shock resistance of two kinds of CLCPs was evaluated in terms of the impact times that the ceramic layer produced crack under 25 J impact energy of a steel ball in 50 mm diameter. The impact locations were chosen at the centers and the edge ends of 200 mm long CLCPs, respectively.

3 Results and Discussion

3.1 Microstructures of Al_2O_3 and ZTA Ceramic Layers

The morphology and phase constituents of 3 mol% Y_2O_3-doped ZrO_2 powders were analyzed by scanning electron microscope (SEM) and X-ray diffractometer (XRD), as shown in Fig. 3a, b. From Fig. 3a, it can be seen that the size of ZrO_2 powders ranges from 30 to 100 nm. The XRD analysis reveals that there are two phase constituents in ZrO_2 powders, the tetragonal and monoclinic ZrO_2 phases. The amounts of m-ZrO_2 and t-ZrO_2 are calculated to be 32.1 and 67.9 % by Eq. (1), respectively.

The Al_2O_3 and ZTA CLCPs were measured in terms of the thickness of ceramic layer, Fe-rich layer and steel substrate pipe; the results are listed in Table 2. The cross-sectional microstructures of Al_2O_3 and ZTA ceramic layers are shown in Fig. 4a, b, respectively. As can be seen, Al_2O_3 ceramic layer consists of long Al_2O_3 dendrites with an average width of 11.3 μm and spinel-like structure $FeAl_2O_4$ distributed at dendrite boundaries, while the microstructure of ZTA ceramic layer changes considerably after addition of ZrO_2; Al_2O_3 dendrites are refined to a width of about

Table 2 Thickness of ceramic layer, Fe-rich layer and steel substrate pipe for Al_2O_3 and ZTA CLCPs (mm)

Pipe type	Ceramic layer	Fe-rich layer	Steel substrate pipe
Al_2O_3 CLCP	1.70	0.86	5.48
ZTA CLCP	1.78	0.83	5.49

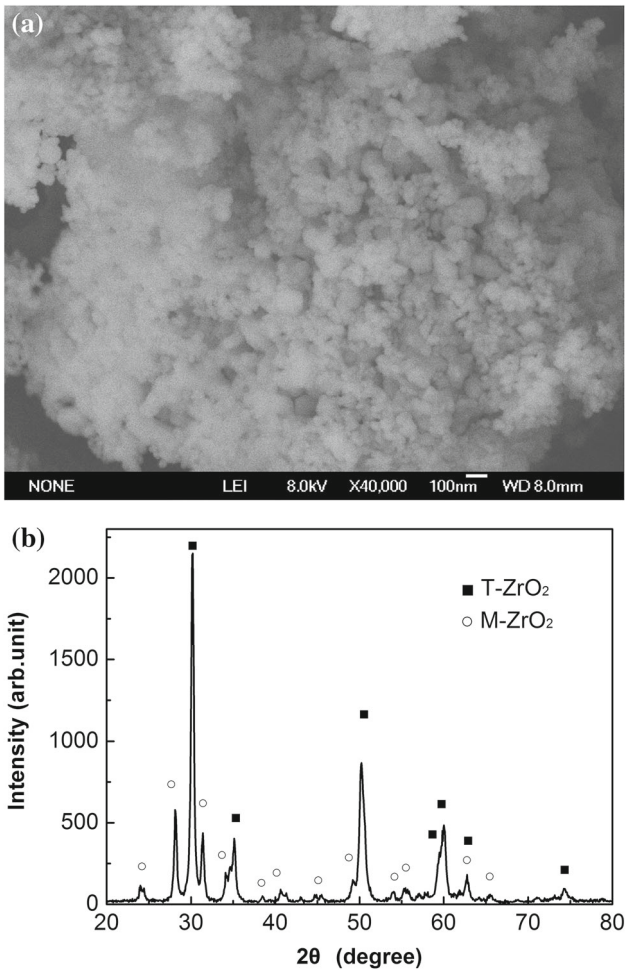

Fig. 3 SEM image (**a**) and XRD pattern (**b**) of 3 mol% Y_2O_3-doped ZrO_2 powders

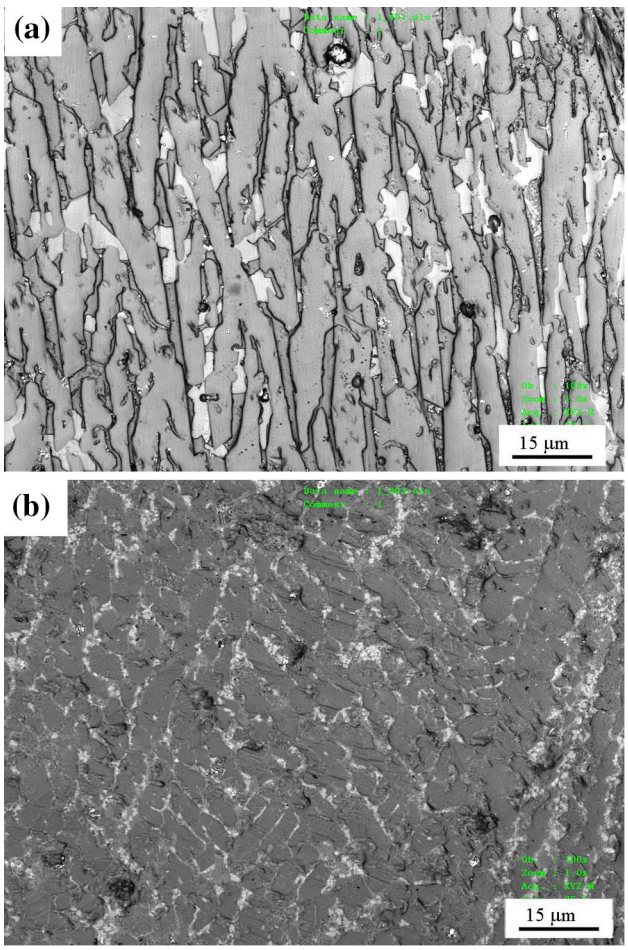

Fig. 4 Optical microstructures of Al_2O_3 (**a**) and ZTA (**b**) ceramic layers

7.7 μm. The refinement of Al_2O_3 dendrites is beneficial to enhancement of fracture toughness to a certain extent. In addition, most of ZrO_2 particles are found to be fine with a size below 1.0 μm and distribute at boundaries of Al_2O_3 dendrites together with $FeAl_2O_4$ phase.

The distribution of fine ZrO_2 particles is not clearly demonstrated in Fig. 4b due to the limited resolution and magnification of the used optical microscope. Therefore, the distributions of ZrO_2 particles and elements in ZTA ceramic layer were further examined using SEM and EDS, as shown in Fig. 5. High-magnification SEM photograph clearly identifies the presence of the fine ZrO_2 particles at boundaries of Al_2O_3 dendrites (Fig. 5a). In addition, oxygen element is found to be distributed homogeneously on the surface

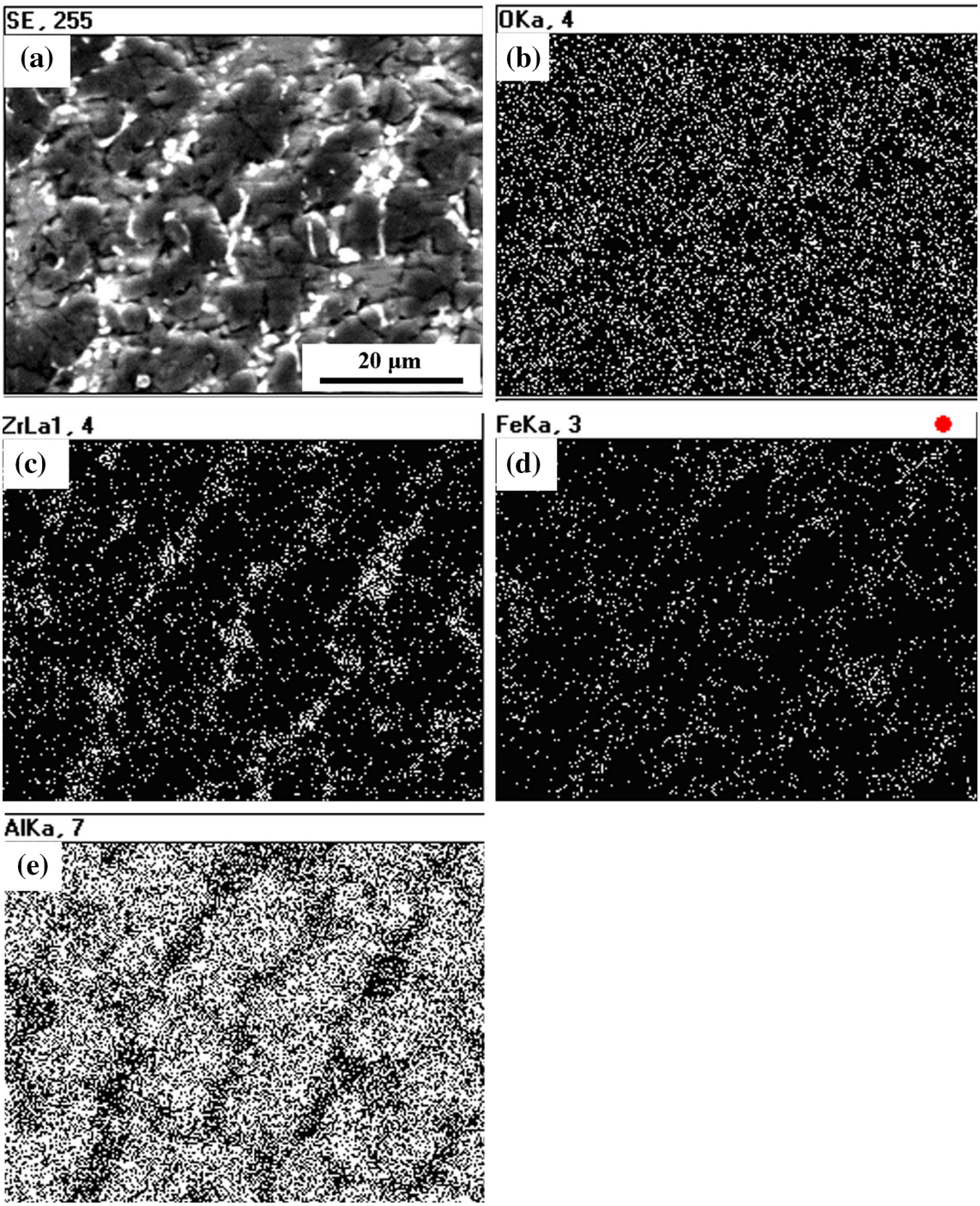

Fig. 5 SEM micrographs and EDS mapping of ZTA ceramic layer: **a** SEM photograph, **b** O, **c** Zr, **d** Fe, **e** Al

since all the three phases in the ceramic layer (Fig. 5b), Al_2O_3, $FeAl_2O_4$ and ZrO_2, contain a high content of oxygen element; hence, no oxygen element aggregation is observed. Zirconium and iron elements are mainly distributed at boundaries of Al_2O_3 dendrites (Fig. 5c, d); the aluminum element is consequently less there (Fig. 5e). This also indicates that both $FeAl_2O_4$ and ZrO_2 are distributed at boundaries of Al_2O_3 dendrites.

Based on the above observations, the microstructures of Al_2O_3 and ZTA ceramic layers may be formed as follows: The melting temperatures of Al_2O_3, $FeAl_2O_4$ and Fe are 2030, 1780 and 1536 °C, respectively. During the solidification of the thermit melt, Al_2O_3 nucleates first and grows toward the heat releasing direction, i.e., along the radius of the pipe, forming the long dendrites. Then $FeAl_2O_4$ eutectic phase begins to form on the boundaries of Al_2O_3 dendrites at about 1750 °C (according to Al_2O_3–FeO binary diagram). After addition of ZrO_2 to the thermit mixture, ZrO_2 powders dissolve into the Al_2O_3 melt during centrifugal-SHS reaction; then in the process of solidification, the Al_2O_3 nucleates first and grows into dendrites until the eutectic temperature of about 1710 °C (according to Al_2O_3–ZrO_2 binary phase diagram), at which the remained melt has already been driven to boundaries of Al_2O_3 dendrites and transforms into the eutectics which mainly contains ZrO_2 and $FeAl_2O_4$ phases.

XRD patterns of Al_2O_3 and ZTA ceramic layers are presented in Fig. 6. The XRD results indicate that Al_2O_3 ceramic layer is comprised of Al_2O_3 and $FeAl_2O_4$ phases, while ZTA ceramic layer consists of Al_2O_3, $FeAl_2O_4$ and t-ZrO_2 phases, and no m-ZrO_2 phase is detected. This is an interesting phenomenon because the raw ZrO_2 powders consist of two phases, m-ZrO_2 and t-ZrO_2, and m-ZrO_2 phase can be detected more or less if the powder mixture of Al_2O_3 and ZrO_2 stabilized by 3 mol% Y_2O_3 is sintered into ZTA ceramics in conventional method [21,22]. The presence of a complete t-ZrO_2 phase in ceramic layer can significantly improve the fracture toughness. This might be related to the solidification features of CLCP produced by SHS CT method. In the process of SHS-centrifugal casting, the cooling velocity of CLCP is rather high, and the ceramic melt solidifies first into ceramic layer due to its higher melting temperature and then followed by Fe-rich melt. The steel pipe and Fe-rich layer have higher coefficient of thermal expansion than the ceramic layer; therefore, a large compressive stress is produced in ceramic layer. This could be the main reason that a complete t-ZrO_2 phase remains in the ceramic layer after SHS-centrifugal casting. It has been reported that the transformation from tetragonal → monoclinic phase can be delayed below room temperature when the ZrO_2 particles are smaller than the critical size of 0.7 μm and subjected to a large compressive strain in the Al_2O_3 matrix. Wang and Yang [23] analyzed the temperature distribution and transformation during the cooling process of the CLCP preparation with finite element numerical simulation; they found a large compressive stress of 152.22 MPa produced in the Al_2O_3 ceramic layer.

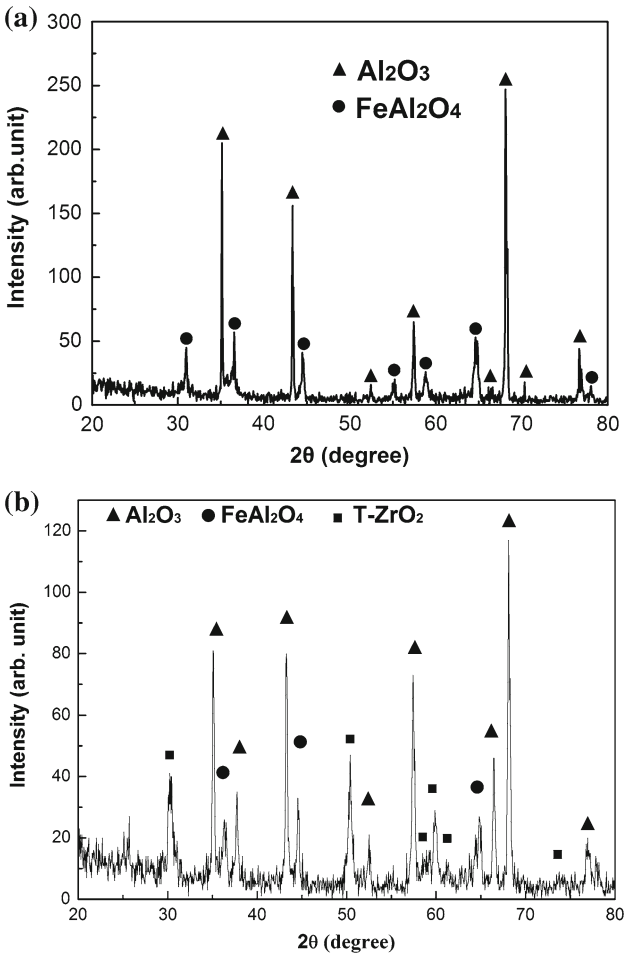

Fig. 6 XRD patterns of Al_2O_3 (**a**) and ZTA (**b**) ceramic layers

3.2 Hardness and Crushing Strength of Al_2O_3 and ZTA CLCPs

The average Vickers hardness values were measured at the centers of ceramic layers, Fe-rich layers and substrates of steel pipes on the cross sections, respectively. In both cases, the ceramic layer is the highest in hardness; the Fe-rich layer is a little lower than the steel substrate of pipe. The low hardness in Fe-rich layer is due to its very low carbon content because a very thin layer of inner surface of steel pipe may melt and dissolve into Fe-rich layer in the process of centrifugal-SHS reaction. It is also found that there is almost no difference in the hardness values of Fe-rich layers or steel pipes between two kinds of CLCPs. The hardness values of Fe-rich layers and steel pipes are about 200 HV and 220 for Al_2O_3 and ZTA CLCPs, whereas the hardness reduced from 1300 HV for Al_2O_3 ceramic layer to 1170 HV for ZTA ceramic layer. This is apparently because ZrO_2 is a little softer than the Al_2O_3 matrix.

The radial crushing load versus displacement curves of two kinds of CLCPs were measured using MTS810 material test system, as shown in Fig. 7. Two horizontal stages occurred one after another on the two curves. Our observation reveals that the first one corresponds to the yield deformation at top and bottom locations of the steel pipe substrate; the second one corresponds to the yield deformation at left and right corners of steel pipe substrate. The ceramic layer begins to crack first at the top and bottom locations when the curve turns into the rising stage, and then cracks at left and right locations when the curve turns into a rapid drop. Therefore, the intersection point of the second horizontal stage and rising stage represents the compression resistance of a ceramic-lined composite steel pipe. The second stages of Al_2O_3 and ZTA ceramic-lined composite pipes are very close to each other in Fig. 7, indicating that addition of ZrO_2 in Al_2O_3 matrix has only little influence on the crushing strength in the present study. In fact, in the compressive testing process, the radial compressive load is mainly undertaken by the steel pipe substrate. In fact, in the compressive testing process, the radial compressive load is mainly undertaken by the steel pipe substrate. Addition of ZrO_2 in Al_2O_3 matrix can significantly change the microstructure and mechanical properties of the ceramic layer, but cannot greatly change the microstructure and properties of steel substrate pipe. The calculated crushing strength values were 354.1 and 365.9 MPa for Al_2O_3 and ZTA CLCPs using Eqs. (3) and (4), respectively. Zhu et al. [24] also obtained a high crushing strength of CLCP by adding nano-ZrO_2 particles in the thermit powder mixtures and ascribed the improvement of crushing strength to the combined effects of refinement of Al_2O_3 dendrites and restriction of crack propagation during cooling period, which originated from tetragonal → monoclinic martensite transformation toughening of fine ZrO_2 particles.

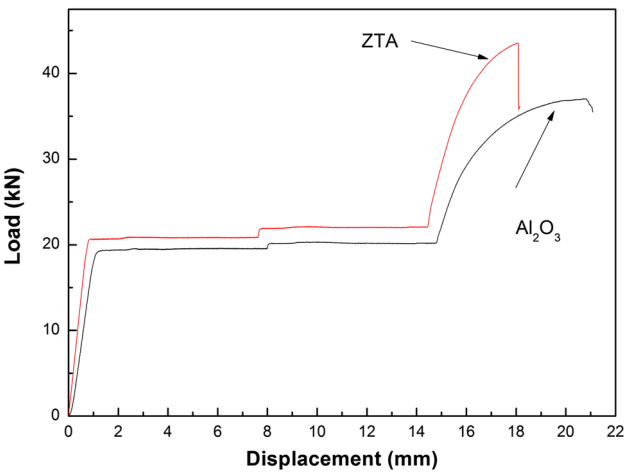

Fig. 7 The radial crushing load versus displacement curves of Al_2O_3 and ZTA CLCPs

3.3 Fracture Toughness and Mechanical Shock Resistance of Al_2O_3 and ZTA CLCPs

The fracture toughness of Al_2O_3 and ZTA ceramic layers is measured by Vickers indentation microfracture method. The fracture toughness is significantly improved by 925 %, increasing from 0.56 MPa $m^{1/2}$ of Al_2O_3 ceramic layer to 5.74 MPa $m^{1/2}$ of ZTA ceramic layer. The crack extension paths were observed under optical microscope after indentation tests, as shown in Fig. 8. It notes that the cracks mainly initiated at top and bottom corners of indention for Al_2O_3 ceramic layer and extended mainly along the growth direction of Al_2O_3 columnar dendrites (Fig. 8a), whereas the cracks initiated at all four corners of the indentation for ZTA ceramic layer and extended in the parallel and perpendicular directions to growth direction of Al_2O_3 columnar dendrites (Fig. 8b). In order to identify the dominant toughening mechanism operating in ZTA ceramic layer, a comparison was made between XRD pasterns of the polished and fractured surfaces (not shown here). It is found that about 33.4 vol% of

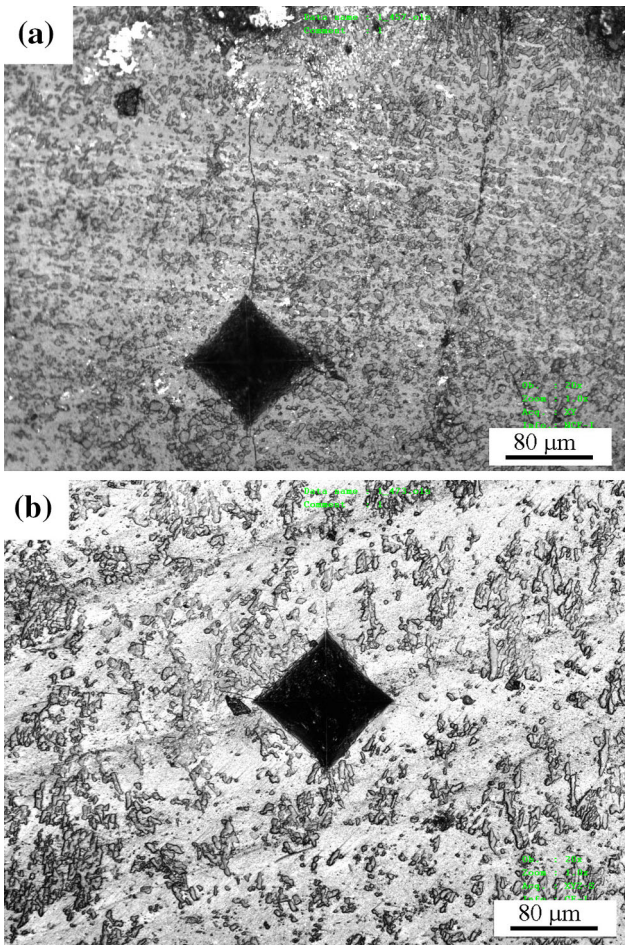

Fig. 8 Crack extension paths induced by indentation: **a** Al_2O_3 layer, **b** ZTA layer

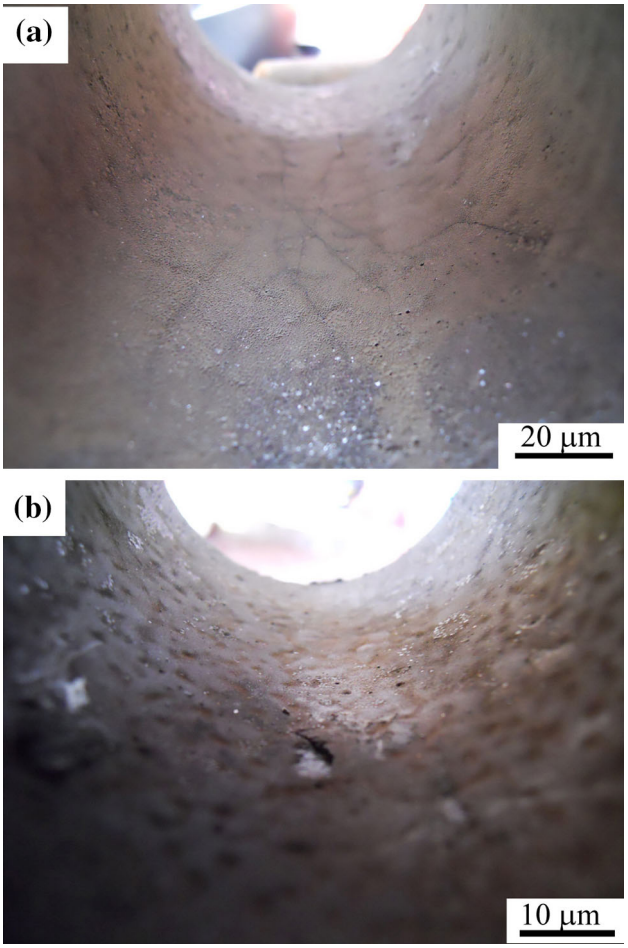

Fig. 9 Inner surface morphologies of Al_2O_3 (**a**) and ZTA (**b**) ceramic layers after mechanical shock tests

t-ZrO_2 phase transformed into m-ZrO_2 phase after fracture. Therefore, the main toughening mechanism is the stress-induced transformation toughening.

The mechanical shock resistance of two kinds of CLCPs was measured under 25 J impact energy of a steel ball in 50 mm diameter. The impact times that the ceramic layer is observed to crack are summarized as follows: The ceramic layer of Al_2O_3CLCP began to crack after only twice impacts at the center of pipe, and the edge can tolerated four times impacts. In contrast, the ceramic layer of ZTA CLCP could bear 19 times impacts at the center and 16 times impacts at the edge, indicating that addition of ZrO_2 in Al_2O_3 matrix can largely improve the mechanical shock resistance of Al_2O_3 ceramic-lined composite steel pipe, and improvements are 850 % at the center and 300 % at the edge, respectively. The inner surfaces of two kinds of CLCPs after impact test at the centers are shown in Fig. 9. After twice impacts, cracks initiated at the impact location on Al_2O_3 CLCP and propagated radially a rather long distance up to 50 mm, whereas after 19 times impacts, only a small spallation of 5 mm emerged at the impact location on ZTA CLCP. Moreover, no crack was observed to be formed around the spallation location. This suggests that addition of ZrO_2 in the Al_2O_3 matrix can greatly resist the propagation of crack in the ceramic layer. The improvement of mechanical shock resistance of the CLCPs brings them convenience to the subsequent procedures such as machining, transportation and installation.

4 Conclusions

- ZTA CLCP was fabricated by centrifugal-SHS technique. The phase constituents of ZTA ceramic layer were Al_2O_3, $FeAl_2O_4$ and t-ZrO_2 phases, and no m-ZrO_2 phase was detected by XRD.
- After addition of ZrO_2 in Al_2O_3 matrix, Al_2O_3 dendrites decreased in width and fine ZrO_2 particles were found to be distributed at dendrite boundaries.
- The hardness of ceramic layer slightly decreased, but the crushing strength was increased a little after addition of ZrO_2 in Al_2O_3 matrix.
- The fracture toughness of ceramic layer was significantly enhanced; the mechanical shock resistance of CLCP was also greatly improved after addition of ZrO_2 in Al_2O_3 matrix.

Acknowledgments The authors wish to express their gratitude for the support under the Project 985-automotive engineering of Jilin University and Natural Science Foundation of Jilin Province (Grant No. 20130102020JC).

References

1. Parkin, I.P.; Elwin, G.M.; Kuznetsov, V.; Pankhurst, Q.A.; Bui, Q.T.; Forst, G.D.; Barquin, L.F.; Komarov, A.V.; Morozov, Y.G.: Self-propagating high temperature synthesis of $MeFe_{12}O_{19}$ (M = Sr, Ba) from the reactions of metal superoxides and iron metal. J. Mater. Process. Technol. **110**, 239 (2001)
2. Munir, Z.A.: Synthesis of high temperature materials by self-propagating combustion method. Am. Ceram. Soc. Bull. **67**, 342 (1988)
3. Munir, Z.A.; Anselmi-Tamburini, U.: Self-propagating exothermic reactions: the synthesis of high-temperature materials by combustion. Mater. Sci. Eng. Rep. **3**, 277 (1989)
4. Seshadri, R.: Centrifugal force assisted combustion synthesis of intermetallics (NiAl). Mater. Manuf. Process. **17**, 501 (2002)
5. Odawara, O.; Shiraishi, M.; Ikeuchi, J.; Ishii, Y.; Yanmasaki, H.; Sato, M.: Characteristics of thermit reaction in a centrifugal-thermit process. J. Jpn. Inst. Met. Mater. **49**, 806 (1985)
6. Odawara, O.: Long ceramic-lined pipes produced by a centrifugal-thermit process. J. Am. Ceram. Soc. **73**, 629 (1990)
7. Underwood, J.H.; Parker, A.P.: Stress and fracture analysis of ceramic lined, composite or steel jacketed pressure vessels. ASME J. Press. Vessels Technol. **126**, 485 (2004)
8. Zhu, Y.; Sun, S.; Ni, H.; Huang, M.: Study on microstructure and properties of ceramic-lined composite steel pipes produced by centrifugal-SHS process. Key Eng. Mater. **464**, 434 (2011)

9. Merzhanov, A.G.: Thermally coupled SHS reactions. Int. J. Self Propag. High Temp. Synth. **20**, 61 (2011)
10. Claussen, N.: Fracture toughness of Al_2O_3 with an unstabilized ZrO_2 dispersed phase. J. Am. Ceram. Soc. **59**, 49 (1976)
11. Shin, D.W.; Orr, K.K.; Schubert, H.: Microstructure-property relationship in hot isostatically pressed alumina and zirconia-toughened alumina. J. Am. Ceram. Soc. **73**, 1181 (1990)
12. Evans, A.G.: Perspective on the development of high-toughening ceramics. J. Am. Ceram. Soc. **73**, 187 (1990)
13. Kaya, C.; Bulter, E.G.: Zirconia-toughened alumina ceramics of helical spring shape with improved properties from extruded sol-derived pastes. Scr. Mater. **48**, 359 (2003)
14. Rao, P.G.; Iwasa, M.; Tanaka, T.; Kondoh, I.; Inoue, T.: Preparation and mechanical properties of Al_2O_3-15 wt%ZrO_2 composites. Scr. Mater. **48**, 437 (2003)
15. Garive, R.C.; Hannink, R.; Pascoe, H.J.R.T.: Ceramic steel?. Nature (London) **258**, 703 (1975)
16. Becher, P.F.: Toughening behavior in ceramics associated with the transformation of tetragonal ZrO_2. Acta Metall. **34**, 1885 (1986)
17. Wang, J.; Stevens, R.: Zirconia-toughened alumina (ZTA) ceramics. J. Mater. Sci. **24**, 3421 (1989)
18. Haward, C.J.; Kisi, E.H.: Polymorph method determination of monoclinic zirconia in partially stabilized zirconia. J. Am. Ceram. Soc. **73**, 3096 (1990)
19. Odawara, O.; Ikeuchi, J.: Study on composite materials with a centrifugal-thermit process. J. Jpn. Inst. Metals **45**, 316 (1981)
20. Nihara, K.; Morena, R.; Haaaelman, D.P.H.: Evaluation of K_{Ic} of brittle solids by the indentation method with low crack-to-indent ratios. J. Mater. Sci. Lett. **1**, 13 (1982)
21. Casellas, D.; Rafols, I.; Llanes, L.; Anglada, M.: Fracture toughness of zirconia–alumina composites. Inter. J. Refract. Met. Hard Mater. **17**, 11 (1999)
22. Casellas, D.; Nagl, M.M.; Llanes, L.; Anglada, M.: Fracture toughness of alumina and ZTA ceramics: microstructural coarsening effects. J. Process. Technol. **143–144**, 148 (2003)
23. Wang, Y.F.; Yang, Z.G.: Finite element analysis of residual thermal stress in ceramic-lined composite pipe by centrifugal-SHS. Mater. Sci. Eng. A **460–461**, 130 (2007)
24. Zhu, Y.; Huang, F.; Sun, S.G.; Ni, H.J.: Effects of nano-reaction system on properties of the superficial ceramic layer of ceramic-lined composite steel pipes. Surf. Technol. **40**(6), 4–6 (2011)